# Pressure-dependent susceptibility of singlet-ground-state paramagnets: Pr and Tm monopnictides and Pr monochalcogenides

R. P. Guertin*
*Physics Department, Tufts University, Medford, Massachusetts 02155*

J. E. Crow†
*Physics Department, Temple University, Philadelphia, Pennsylvania 19122*

L. D. Longinotti and E. Bucher‡
*Bell Laboratories, Murray Hill, New Jersey 07974*

L. Kupferberg
*Department of Physics and Astronomy, University of Rochester, Rochester, New York 14627*

S. Foner
*Francis Bitter National Magnet Laboratory,§ Massachusetts Institute of Technology, Cambridge, Massachusetts 02139*
(Received 24 February 1975)

Measurements of the pressure dependence (up to $\sim 6$ kbar) of the magnetic susceptibility $\chi$ at 4.2 K are presented for three Pr monopnictides (PrAs, PrSb, and PrBi), two Tm monopnictides (TmAs and TmSb), and three monochalcogenides (PrS, PrSe, and PrTe). The results for $(1/\chi)\,(d\chi/dP)$ in units of $10^{-3}$ kbar$^{-1}$ are: PrAs $+10$; PrSb, $+7$; PrBi, $+9$; TmAs, $+6$; TmSb, $+3$; PrSe, $-2$; and PrTe, $-1$; for PrS, $(1/\chi)(d\chi/dP)$ is nonmonotonic, but negative. Independent inelastic-neutron-scattering data, which show that for all the materials studied the crystalline electric field (CEF) of the surrounding ions produces a nonmagnetic (singlet) ground state with a magnetic (triplet) first excited state, are employed for analysis of the present experiments. None of the compounds studied orders magnetically; the susceptibility is Van Vleck like, and is nearly temperature independent at 4.2 K. For both sets of monopnictides, the susceptibility increases under pressure, whereas the point-charge model, which has been used previously to explain the CEF splittings, always predicts a decrease. For the monochalcogenides, the susceptibility decreases slightly, consistent with the predictions of the point-charge model. The results are discussed in terms of the predictions of the point-charge model, the pressure dependence of the enhancement, and other possible mechanisms.

## I. INTRODUCTION

The interaction of the rare-earth ion with its surrounding crystalline electric field has been studied in many rare-earth intermetallic compounds.[1-5] In these compounds the crystalline electric field (CEF) of the neighboring ions partially lifts the $2J+1$ degeneracy of the rare-earth ground state given by Hund's rule. Of particular interest in this paper are those compounds for which the lowest-lying rare-earth CEF sublevel is a nonmagnetic level, i.e., a singlet or nonmagnetic doublet. This can occur when the rare-earth ion possesses an even number of $4f$ electrons (Kramer's theorem), i.e., Pr ($J=4$), Tb and Tm ($J=6$), and Ho ($J=8$). For the rare-earth compounds reported in this paper, neutron scattering experiments[2,3] show that the splitting between the ground and first excited state, $\Delta$, is typically 25–150 K. Hence, for $T \ll \Delta$, only the nonmagnetic ground state is thermally populated and magnetic ordering can occur only if a critical ratio between the exchange interaction and CEF energy is exceeded.[6,7] Frequently, this criterion is not satisfied, so that the compounds do not order magnetically at any temperature.

Several experimental techniques, e.g., susceptibility,[8] specific heat,[8] electron paramagnetic resonance,[9] and thermoelectric power,[10] have been used with varying success to determine the CEF level structure of rare-earth compounds and alloys. Inelastic neutron scattering[1-3] yields the most direct determination, at least in intermetallic compounds. Surprisingly, the observed crystal-field level splittings for many of the compounds discussed in this paper are very similar to those predicted by an unscreened point-charge model (PCM)[11] for crystalline electric fields. In this model the electric field is presumed to arise solely from point charges located at the sites of neighboring atoms. No provision is made in the PCM for conduction-electron screening or covalency.[12]

For those singlet-ground-state rare-earth compounds that do not order magnetically, the magnetic susceptibility at low temperatures, $T \ll \Delta$, is due to an admixture of excited CEF states with the ground state.[4] This crystal-field-only Van Vleck type paramagnetism can be calculated exactly if the CEF energies are known and the spin-spin interaction between rare-earth ions is neglected. Furthermore, within the framework of

the PCM, the dependence on lattice spacing of the crystal-field-only susceptibility can be predicted, which is of particular interest for our hydrostatic-pressure measurements. In most of the cases examined below, the observed susceptibility at $T \ll \Delta$ exceeds the crystal-field-only value; this indicates the presence of paramagnetic contributions to the susceptibility which are not CEF in origin.

In this paper we report the effect of hydrostatic pressure on the low-temperature magnetic susceptibility of several Pr pnictides (PrAs, PrSb, and PrBi), Tm pnictides (TmAs and TmSb), and Pr chalcogenides (PrS, PrSe, and PrTe). None of these compounds order magnetically and the CEF level structure for all these materials have been well characterized by inelastic neutron scattering.[2,3] Consequently, in all cases the crystal-field-only susceptibility can be calculated (within the accuracy of the neutron scattering results). Based on the PCM, we expect the CEF splitting to increase under pressure as the neighboring charges are brought closer to the rare-earth ion. Low-temperature susceptibility measurements under hydrostatic pressure are ideally suited to probe this behavior. In many cases, however, it is found that the behavior predicted by the PCM is not observed.

In Sec. II we describe the experimental procedures and sample preparation. In Sec. III we review the CEF Hamiltonian, the point-charge model, and the predictions of the PCM for the pressure dependence of the low-temperature magnetic susceptibility. In Sec. IV we present the experimental results and compare them with the crystal-field-only point-charge-model predictions. Finally we discuss the results including the effects of exchange.

## II. EXPERIMENTAL DETAILS

### A. Magnetic measurements under hydrostatic pressure

The method of measuring the hydrostatic pressure dependence of the susceptibility has been described in detail elsewhere.[13] An exploded view of the salient parts of the apparatus is shown in Fig. 1. Briefly the method is as follows: Pressure is applied with a small beryllium-copper self-locking clamp device[14] (CB and associated parts) which is attached to the end of the drive rod (H) of a commercial vibrating-sample magnetometer.[15] The entire clamp-plus-sample assembly is oscillated at ~90 Hz in a homogeneous (one part in $10^4$ over a 3-cm-diam sphere) 7-T Nb-Ti superconducting solenoid (M). The magnetic moment of both clamp and sample are detected by series-opposing pickup coils (PC) located inside the solenoid.

The sensitivity of this method is ~$10^{-3}$ emu, which is adequate for detecting small pressure-induced changes of a few percent in the magnetization of the ~10-mg samples discussed here. The sensitivity of the vibrating-sample magnetometer (with these large pickup coils) when used for ordinary zero-pressure experiments is ~$10^{-5}$ emu. The reduced sensitivity in pressure-related experiments is caused by the spurious signal from eddy currents induced in the metallic clamp body as it moves rapidly through small field inhomogeneities. The background of the clamp (which often outweighs the sample by ~$10^3$:1) is typically ~$10^{-2}$ emu at the highest fields used. Since the clamp must be removed from the cryostat and warmed up to room temperature in order to change pressures, the largest error in the magnetization-vs-pressure data arises from the inability of positioning reproducibly the sample (plus clamp) from run to run. The resolution of the measured signal in a run at

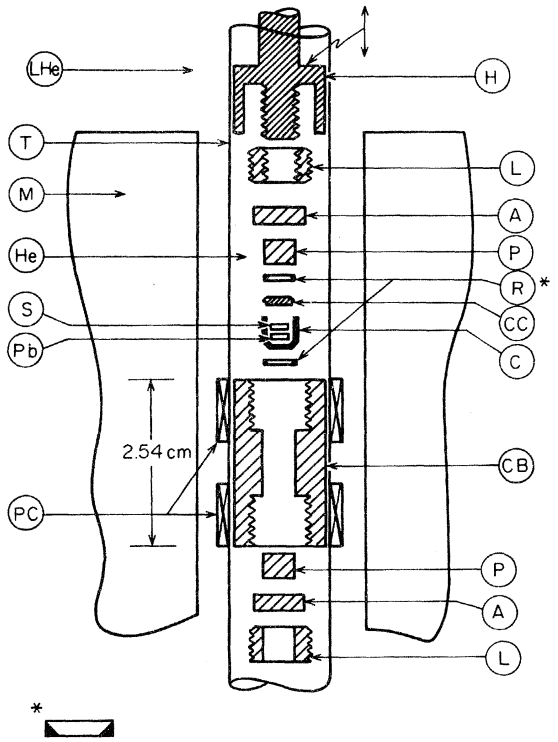


FIG. 1. Exploded view of the beryllium-copper hydrostatic-pressure clamp assembly in the superconducting solenoid. The components are: LHe—liquid-helium reservoir; T—stainless-steel tube containing helium exchange gas (He); M—7-T Nb–Ti superconducting solenoid; S—sample; Pb—lead disk, used occasionally for pressure calibration (ordinarily a Sn disk is used); CB—clamp body; PC—pickup coils; H—clamp holder, connected to the drive rod of the magnetometer; L—locking screws; A—anvils; P—pistons; R—retaining rings; CC—Teflon capsule cover; C—Teflon capsule filled with pressure-transmitting fluid (1:1 isoamyl alcohol and *n*-pentane). (After Ref. 13.)

fixed pressure was $\lesssim 0.1\%$ in all cases. The uncertainty in the magnetization was estimated by running each sample in the clamp at zero pressure at least twice. In all cases this uncertainty was found to be better than 1% of the measured signal, whereas most of the pressure-induced changes in magnetization were a few percent. Between one and six high-pressure measurements were made on each sample in addition to the zero-pressure measurements.

The magnetization at 4.2 K for each sample was also measured to ~5 T at atmospheric pressure in the absence of the clamp. In all cases the magnetization showed a slight curvature at high fields. This was expected due to field-induced mixing of excited magnetic CEF levels with the singlet ground state. The curvature was most pronounced in those samples with the smallest $\Delta$, also as expected. Most of the pressure-dependent data were taken at low fields, where the magnetization was linear with field (up to ~3 T for some of the Pr compounds and up to ~1.5 T for the Tm compounds).

The low-temperature hydrostatic pressure $P$ was calibrated in a separate experiment after each of the runs described above. This was accomplished by measuring the shift in the superconducting transition temperature $T_c$ of a Sn disk,[16] which was included with the sample in the pressure capsule at all times. After each run at fixed pressure, the $T_c$ of the Sn at zero field was measured in a cryostat designed for this purpose using a modified ac susceptibility technique.[17] This method allows determination of $P$ to within a few percent. Any changes with pressure in the shape of the Sn transition curve are indicative of nonideal hydrostatic pressure; no such changes were observed in any of our measurements. Thus in all of the data reported here the pressure was truly hydrostatic.

### B. Sample preparation

Rare-earth antimonides and bismuthides were prepared by direct fusion of the components in a tantalum tube (0.8–1.0-cm diameter, 0.02-cm wall). Small pieces of the constituents were mixed in the tube and reacted together by resistance heating. The ends of the tube were folded twice and clamped in a heavy-current clamp. In this way the stoichiometry was guaranteed; no sublimation effects were observed on the cold side of the tube. The tube was turned over and the sample remelted to ensure homogeneity. After the second melting step, the liquid was cooled slowly (200–400 °C/min). Solidification occurred first at the bottom of the tube; sometimes large single crystals of 3- to 9-mm diameter can be obtained in this way.

Stoichiometric rare-earth arsenides and phosphides cannot be grown in the manner described above. Therefore, chips or filings of the components were completely prereacted in a sealed quartz tube (ordinarily for 2 or 3 d at temperatures of 900 °C). The reaction product was then crushed in dry nitrogen, pressed into pills, and subsequently reacted at 1000 °C for 1 to 2 d. The pills were then transferred to a tungsten crucible, electron-beamed sealed, and fired for several days at 2000–2200 °C in a small temperature gradient, with the pills located in the coolest section of the crucible. In this way single crystals or large polycrystalline sections can be grown from the pills.

## III. THEORY OF CRYSTALLINE-ELECTRIC-FIELD EFFECTS FOR Pr AND Tm MONOPNICTIDES AND Pr MONOCHALCOGENIDES

### A. Crystal-field Hamiltonian and point charge model

The crystal-field Hamiltonian appropriate for a site of cubic symmetry may be written[11]

$$H_{CEF} = A_4\langle r^4\rangle \chi_4 (O_4^0 + 5O_4^4) + A_6\langle r^6\rangle \chi_6 (O_6^0 - 21O_6^4). \tag{1}$$

Here the coefficients $A_4$ and $A_6$ are factors which determine the scale of the crystal-field splittings. The terms $\langle r^4\rangle$ and $\langle r^6\rangle$ are the mean fourth- and sixth-order powers, respectively, of the radii of the magnetic ($4f$) electron wave functions. $\chi_4$ and $\chi_6$ are reduced matrix elements appropriate to the particular $J$ value of the rare-earth ion ($J=4$ for Pr and $J=6$ for Tm), and finally, $O_n^m$ are the Stevens operator equivalents.

Lea, Leask, and Wolf[18] (LLW) have rewritten the CEF Hamiltonian in a slightly modified form:

$$H_{LLW} = W\left(x\,\frac{O_4}{F(4)} + (1-|x|)\,\frac{O_6}{F(6)}\right), \tag{2}$$

where $W$ is a scale factor determining the over-all CEF splitting, $O_4$ and $O_6$ are the fourth- and sixth-order operator combinations shown in the parentheses of Eq. (1), and $x$ ($-1 \le x \le 1$) determines the relative strength of fourth- and sixth-order terms:

$$\begin{aligned} Wx &= A_4\langle r^4\rangle \chi_4 F(4)\,, \\ W(1-|x|) &= A_6\langle r^6\rangle \chi_6 F(6)\,. \end{aligned} \tag{3}$$

The terms $F(4)$ and $F(6)$ are numerical factors for a given value of $J$. LLW have diagonalized the Hamiltonian [Eq. (2)] and have determined the CEF eigenvalues and eigenvectors as a function of $x$ for various values of $J$. In Figs. 2 and 3 we show the eigenvalues which result from this diagonalization for $J=4$ (Pr compounds) and $J=6$ (Tm compounds), respectively. The vertical scale is in arbitrary energy units. For each diagram we have indicated the range of $x$ appropriate to the Pr and Tm compounds studied, as determined from the results of inelastic-neutron-scattering experiments.[2,3] Note that in both cases there is a $\Gamma_1$ (singlet) ground state and a $\Gamma_4$ (magnetic triplet) first excited state.

Within the framework of a point-charge model (PCM) the coefficients $A_4\langle r^4\rangle$ and $A_6\langle r^6\rangle$ are[11] (for the sixfold coordination appropriate to the NaCl structure)

$$A_4\langle r^4\rangle = \tfrac{7}{16}(Ze^2/R^5)\langle r^4\rangle$$

and

$$A_6\langle r^6\rangle = \tfrac{3}{64}(Ze^2/R^7)\langle r^6\rangle \ , \qquad (4)$$

where a point charge $Ze$ is assigned to each nearest-neighbor ion, each of which is separated by a distance $R$ from the rare-earth ion. It is found that the PCM gives quantitatively satisfactory agreement with the observed CEF level structure in most cases of the Pr pnictides and chalcogenides when an effective charge of about $-2e$ is assigned to the nearest neighbors. This result is quite surprising because there is no provision in this model for taking into account conduction-electron screening and covalency effects.[12]

### B. Magnetic susceptibility

The magnetic susceptibility due to CEF effects, $\chi$, for the compounds studied is given at all temperatures by[4]

$$\chi = \chi_R + \chi_P \ , \qquad (5)$$

where $\chi_R$ is that part which arises from the thermal population changes caused by the magnetic field between states which have a magnetic moment in the absence of field. At low temperatures, where only the nonmagnetic singlet is thermally populated, $\chi_R \to 0$ and the low-field susceptibility in the absence of spin-spin interactions is given by $\chi_P$, which is the crystal-field-only Van Vleck-type susceptibility, and can be written[4]

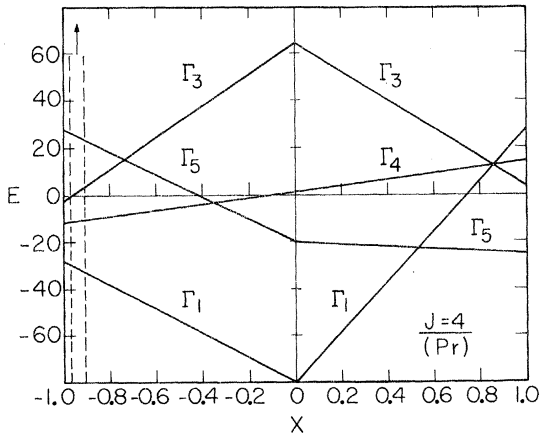


FIG. 2. Eigenvalues of the CEF Hamiltonian [Eq. (2)] for $J=4$ (appropriate for Pr). The dashed lines indicate the range of $x$ for the Pr compounds studied; the arrow indicates the direction of increasing energy of the CEF levels ($\Gamma_1$ singlet is ground state and $\Gamma_4$ triplet is first excited state). (After Ref. 18.)

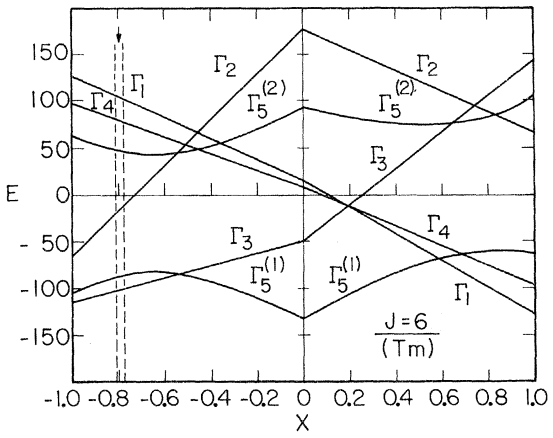


FIG. 3. Eigenvalues of the CEF Hamiltonian [Eq. (2)] for $J=6$ (appropriate for Tm). The dashed lines indicate the range of $x$ for the Tm compounds studied; the arrow indicates the direction of increasing energy of the CEF levels, i.e., $\Gamma_1$ is the lowest level. (After Ref. 18.)

$$\chi_P(T=0, H=0) \equiv \chi_c = \frac{2g^2\mu_B^2 |\langle \Gamma_4 | J_z | \Gamma_1 \rangle|^2}{k_B \Delta} \ , \qquad (6)$$

where $g$ is the Landé $g$ factor, $\mu_B$ is the Bohr magneton, and $\Delta$ has been defined above. The matrix elements of the magnetic moment ($J_z$) operator between the ground-state eigenvector $|\Gamma_1\rangle$ and the excited state eigenvectors vanish with the exception of the first excited state $|\Gamma_4\rangle$.

Using the PCM, the hydrostatic-pressure dependence of $\chi_c$ can be predicted. Naively, we expect that as the nearest-neighbor charges are brought closer to the rare-earth ions, the CEF interaction and hence $\Delta$ will *increase*. [In the PCM this comes about through a reduction of the denominators of $A_4\langle r^4\rangle$ and $A_6\langle r^6\rangle$; see Eq. (4).] Then the susceptibility should *decrease* because of the larger denominator of Eq. (6). Assuming that $x < 0$, that only $\Gamma_1$ and $\Gamma_4$ are involved (which is the case for compounds discussed here), and that $\Gamma_1$ and $\Gamma_4$ depend linearly on $x$ (which is true for $J=4$ and $J=6$ as shown in Figs. 2 and 3), the pressure dependence of $\chi_c$ is given by

$$\frac{1}{\chi_c}\frac{d\chi_c}{dP} = -\frac{\kappa}{3}\left(5 + \frac{2\Delta_0(1+x)}{\Delta}\right) \ , \qquad (7)$$

where $\kappa$ is the compressibility of the material and $\Delta_0$ is the value of $\Delta$ at $x=0$. It is important to note that a *decrease* in susceptibility is always expected, (see note added in proof).

In the discussion above we have assumed that the magnetic susceptibility is entirely due to mixing between the crystal-field levels; i.e., we have neglected spin-spin interactions. In fact, the measured low-temperature susceptibility of our sam-

ples is as much as 25% higher than the crystal-field-only value calculated from Eq. (6) with measured neutron scattering CEF parameters. We attribute this *enhanced* susceptibility to exchange between the rare-earth ions. (Recall that if this exchange is sufficiently large, magnetic ordering at low temperatures may result. This is the case for TbSb,[19] which orders antiferromagnetically at ~16 K, although it is not the case for TmSb, one of the materials discussed in this paper.) The measured (enhanced) susceptibility $\chi_m$ can be written in terms of the crystal-field-only susceptibility $\chi_c$ and the exchange constant $\mathcal{J}$ as[19,20]

$$\chi_m = \frac{\chi_c}{1 - \mathcal{J}\chi_c} \quad . \tag{8}$$

Equation (8) is written in the form of the molecular-field model of induced ferromagnetism.[21] [Induced ferromagnetism occurs at the temperature where the denominator of Eq. (8) vanishes, i.e., for $\mathcal{J} = \chi_c^{-1}$.] Equation (7) does not take account of exchange enhancement. Most of the samples discussed here show an exchange enhancement, so that Eq. (7) is not expected to predict accurately the pressure dependence of $\chi_m$.

## IV. RESULTS AND DISCUSSION

The results of the experiments reported in this paper as well as the results of neutron scattering experiments are summarized in Table I.[22]

### A. Zero-pressure magnetization

The magnetization at 4.2 K with applied field up to ~5 T of all samples was measured in the absence of the pressure clamp. In Figs. 4 and 5 we show these results for two of the samples, PrSb and TmSb, respectively. Also indicated in Fig. 4 is the small, ~4%, increase in magnetization of PrSb observed at the highest applied hydrostatic pressure (see Sec. IV C). The results of inelastic neutron scattering show that the splitting between the ground (singlet) and first excited (triplet) state, $\Delta$, is 71.9 K for[2] PrSb and 24.9 K for[3] TmSb. The dashed lines in Figs. 4 and 5 represent $\chi_c$ derived from these splittings. The greater curvature of the TmSb magnetization compared to the PrSb magnetization is expected, since the smaller the splitting $\Delta$, the greater the amount of field-induced mixing of excited and ground-state levels. The TmSb sample studied was a single crystal, with the field along the [100] axis; all the other samples were polycrystalline. Although the high-field magnetization of crystal-field-only compounds is expected to be anisotropic, the low-field susceptibility for these cubic systems is closely isotropic.[4] Since the pressure experiments reported here cover only the low-field portion of the magnetization, we regard our data as representing the pressure dependence of the low-temperature susceptibility, regardless of whether or not the sample is single crystal or polycrystalline.

In Table I we have listed the crystal-field parameters found from inelastic neutron scattering and the susceptibility $\chi_c$ calculated from these parameters using Eq. (6). The errors indicated for $\chi_c$ reflect the uncertainties of the measured $A_4\langle r^4\rangle$ and $A_6\langle r^6\rangle$ parameters. Also listed are the measured susceptibilities $\chi_m$ (the low-field slope of magnetization curves such as those of Figs. 4 and

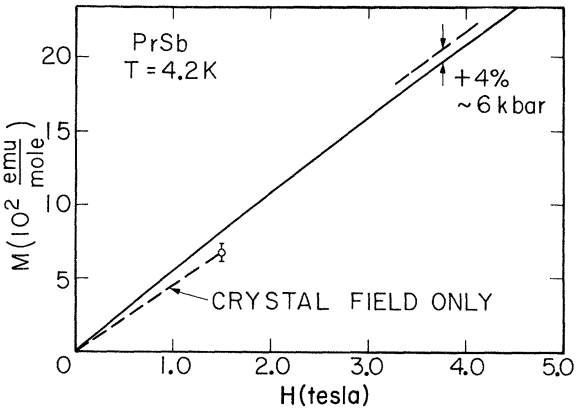


FIG. 4. Magnetization $M$ of PrSb at 4.2 K at atmospheric pressure. The dashed line represents the zero-field crystal-field-only susceptibility $\chi_c$ at $T=0$ calculated from the crystal-field parameters obtained from inelastic-neutron-scattering experiments (Ref. 2). The error bar shows the uncertainty in $\chi_c$ based on uncertainties of the neutron scattering data. Also indicated is the +4% increase in $M$ observed at ~6 kbar.

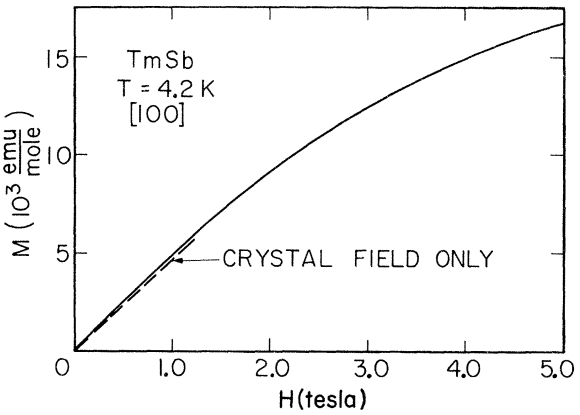


FIG. 5. Magnetization $M$ of single-crystal TmSb along the [100] direction at $T=4.2$ K and atmospheric pressure. The dashed line represents the zero-field crystal-field-only susceptibility $\chi_c$ at $T=0$ calculated from the crystal-field parameters obtained from inelastic-neutron-scattering experiments (Ref. 3). The uncertainty of $\chi_c$ is within the width of the dashed line.

TABLE I. Summary of properties related to the pressure dependence of the susceptibility for Pr and Tm monopnictides and Pr monochalcogenides.

| | Lattice properties | | Neutron scattering properties | | | | | | Pressure-dependent properties | | | | | |
|---|---|---|---|---|---|---|---|---|---|---|---|---|---|---|
| Sample | $a_0$[a] (Å) | $\kappa$[b] ($10^{-13}$ cm$^2$/dyn) | $A_4\langle r^4\rangle$ (meV) | $A_6\langle r^6\rangle$[a] (meV) | $W$[c] (K) | $x$[c] | $\Delta$[c] (K) | $\chi_c$[c,d] ($10^{-2}$ emu/mole) | $\chi_m$[e] ($10^{-2}$ emu/mole) | $\left(\frac{1}{\chi_c}\frac{d\chi_c}{dP}\right)$[f] ($10^{-3}$/kbar) | $\left(\frac{1}{\bar\eta}\frac{d\bar\eta}{dP}\right)$[g] ($10^{-3}$/kbar) | $n$[h] | $\mathcal{J}$[i] (mole/emu) | $\frac{1}{\mathcal{J}}\frac{d\mathcal{J}}{dP}$[i] ($10^{-2}$/kbar) |
| Pr monopnictides | | | | | | | | | | | | | | |
| PrAs | 6.030 | 28 | 12.3 ±0.9 | 0.35 ±0.18 | 6.59 | −0.955 | 133 | 2.41 ±0.30 | 3.82 | −5.1 | +10 | 1 | 15.3 | +3.7 |
| PrSb | 6.376 | 19.6 | 8.3 ±0.3 | 0.17 ±0.07 | 4.40 | −0.966 | 72.1 | 4.44 ±0.47 | 5.32 | −3.5 | +7 | 3 | 3.7 | +5.7 |
| PrBi | 6.461 | 21 | 6.9 ±0.3 | 0.24 ±0.06 | 3.75 | −0.943 | 67.5 | 4.74 ±0.34 | 6.18 | −3.9 | +9 | 3 | 4.9 | +4.6 |
| Tm monopnictides | | | | | | | | | | | | | | |
| TmAs | 5.711 | 24 | 8.55 ±0.15 | 0.53 ±0.06 | −1.231 | −0.788 | 31.3 | 37.3 ±1.3 | 45.9 | −4.1 | +6 | 2 | 0.50 | +4.9 |
| TmSb | 6.084 | 15 | 6.81 ±0.10 | 0.44 ±0.04 | −0.988 | −0.782 | 24.9 | 46.8 ±1.3 | 51.6 | −2.6 | +3 | 1 | 0.20 | +5.7 |
| Pr monochalcogenides | | | | | | | | | | | | | | |
| PrS | 5.735 | 71 | 13.8 +1.6 −3.2 | 0.72 +0.47 −0.25 | 7.76 | −0.911 | 157 | 2.04 ±0.51 | 2.18 | −10.1 | j | 6 | 3.1 | |
| PrSe | 5.942 | 12 | 12.7 +0.27 −0.58 | 0.49 +0.13 −0.18 | 6.86 | −0.948 | 121 | 2.65 ±0.23 | 2.73 | −2.2 | −2 | 2 | 1.1 | |
| PrTe | 6.320 | 32 | 9.1 +2.0 −3.1 | 0.16 +0.08 −0.13 | 4.94 | −0.974 | 78.1 | 4.10 ±1.26 | 4.43 | −5.6 | −1 | 2 | 1.8 | |

[a]Lattice constants, $a_0$ and $A_4\langle r^4\rangle$, and $A_6\langle r^6\rangle$ were taken from Refs. 2 and 3. The uncertainties in $A_4\langle r^4\rangle$ and $A_6\langle r^6\rangle$ reflect the uncertainties in the neutron scattering data.

[b]For a discussion of the compressibility $\kappa$ see Ref. 22.

[c]Values of $W$, $x$, $\Delta$, and $\chi_c$ are calculated from $A_4\langle r^4\rangle$ and $A_6\langle r^6\rangle$.

[d]The uncertainties in $\chi_c$, the calculated low-temperature, zero-field, crystal-field-only susceptibility, reflect the uncertainties of the measured crystal field parameters $A_4\langle r^4\rangle$ and $A_6\langle r^6\rangle$.

[e]$\chi_m$ is the measured low-field susceptibility at 4.2 K.

[f]$(1/\chi_c)(d\chi_c/dP)$ is calculated using Eq. (7).

[g]$(1/\bar\eta)(d\bar\eta/dP)$ is approximately equal to $(1/\chi_m)(d\chi_m/dP)$; see text for details.

[h]$n$ is the number of high pressurizations per sample.

[i]$\mathcal{J}$ is the exchange constant, Eq. (8), and $(1/\mathcal{J})(d\mathcal{J}/dP)$ is obtained from comparison of $(1/\chi_c)(d\chi_c/dP)$ and $(1/\bar\eta)(d\bar\eta/dP)$.

[j]For PrS, $(1/\bar\eta)(d\bar\eta/dP)$ is nonmonotonic, see Fig. 8.

5). Note that in all cases $\chi_m > \chi_c$, and for the Pr and Tm pnictides this difference is greater than the uncertainty in $\chi_c$. We expect other contributions to the susceptibility $\chi_m$, such as Pauli paramagnetism, core diamagnetism, etc., to be very small.[23] We attribute the excess susceptibility to exchange enhancement. The exchange constant $\mathcal{J}$ derived from Eq. (8) is also listed in Table I.

### B. Analysis of the high-pressure data

For each sample the magnetization $M$ vs applied field $H$ at 4.2 K was measured at $P=0$ at least twice with the sample in the hydrostatic-pressure clamp. The second measurement of $M(H, P=0)$ was made after at least one measurement of $M(H, P\neq 0)$ in order to obtain an estimate of the reproducibility of the data from run to run. [As mentioned in Sec. II, differences in $M(H, P=0)$ were smaller than 1%, whereas the pressure-induced changes observed were usually $\gtrsim 1\%$.]

For each pressurization of the sample, the magnetization at constant field was measured at a minimum of ten equally spaced field intervals within the linear $M$-vs-$H$ region. At each fixed field at least ten values of $M$ and $H$ were recorded on an automatic paper-tape logging system. The data for each fixed field were averaged by computer. A fit of the data to the function $M(H, P)=AH+BH^3$ was attempted. However, owing to the spurious background moment of the pressure clamp at low fields, the deviations of the data from this function were found to have systematic trends. Thus it was difficult to resolve unambiguously the variation with pressure of the susceptibility. For example, none of the samples showed a spontaneous magnetic moment when measured outside the clamp but the clamp itself showed a small moment at very low fields. A more satisfactory fit was obtained with a fourth-order polynomial including a constant term.

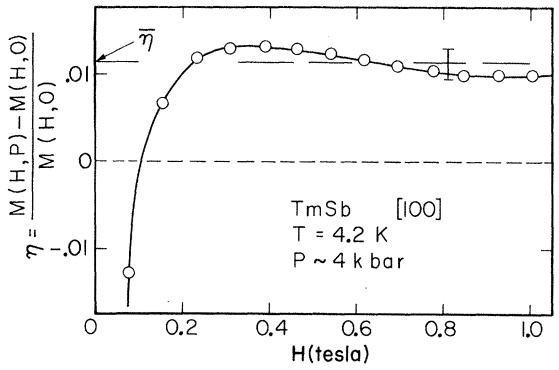


FIG. 6. Relative change of the magnetization $\eta$ for TmSb vs field at 4.2 K and $P=4$ kbar. At very low fields there are large uncertainties in $\eta$ due to the relatively large moment of the clamp background. At higher fields, however, $\eta$ approaches a constant value, $\bar{\eta}$, which is also indicated along with our estimated uncertainty in $\bar{\eta}$, shown by the error bar.

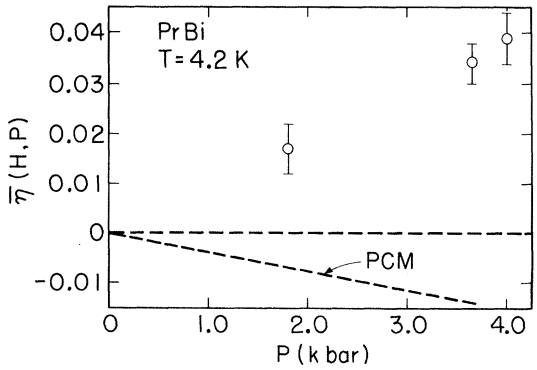


FIG. 7. Value of $\bar{\eta}$ at 4.2 K for PrBi for three high-pressurization runs. Note the large positive increase in $\bar{\eta}$ with pressure, in contrast to the decrease predicted by the point-charge model (indicated by the dashed line).

In order to compare the high-pressure magnetization data with the $P=0$ data, the following expression was calculated:

$$\eta = \frac{M(H,P)-M(H,0)}{M(H,0)} \quad . \tag{9}$$

The fourth-order polynomial was used to calculate $\eta$. This procedure permitted interpolation of $H$ for point-by-point subtraction, since the magnetization data were not collected at exactly the same fixed fields. This polynomial was chosen because it smoothed the data sufficiently without introducing systematic variations from the fitted function. The data were all taken at sufficiently low fields so that the linear term dominated the magnetization data in all cases.

In Fig. 6 we show $\eta$ vs $H$ for one pressurization of TmSb. At very low fields there is large uncertainty due to the relatively large contribution to $M(H, P)$ of the spurious signals mentioned above. At slightly higher fields, however, $\eta$ tends to stabilize. Also indicated in Fig. 6 is the average value of $\eta$, given by $\bar{\eta}$, and our chosen uncertainty in $\bar{\eta}$. As can be seen an increase of $\eta$ with increasing pressure is clearly resolved. [$M(H, P)$ vs $H$ deviated from linearity at the largest $H$ by only a few parts in $10^3$. Therefore the expression $(1/\bar{\eta})(d\bar{\eta}/dP)$ is equal to the relative change with pressure of the measured susceptibility $\chi_m$ to within a few parts in $10^3$.] The data shown in Fig. 6 were characteristic of the data for other samples; however, there was generally somewhat greater scatter at higher fields in the other cases.

In Fig. 7, $\bar{\eta}$ vs $P$ is plotted for three high-pressurization runs of PrBi. An increase of $\bar{\eta}$ with $P$

is clearly seen in Fig. 7. Also plotted is the prediction of the point-charge model (PCM) for PrBi [see Eq. (7)]. Obviously our results for this sample disagree with the predictions of the PCM.

### C. Results of the pressure-dependent susceptibility experiments

#### *1. Pr pnictides (PrAs, PrSb, and PrBi)*

The susceptibility $\chi_m$ of the three Pr pnictides studied is somewhat enhanced over $\chi_c$, the crystal-field-only value (see Table I). In all three cases the measured susceptibility *increases* under pressure [see $(1/\bar{\eta})(d\bar{\eta}/dP)$ in Table I and the data of Fig. 7], whereas the PCM predicts a decrease [see $(1/\chi_c)(d\chi_c/dP)$ in Table I].

The pressure dependence of $\bar{\eta}$ could be caused by an increase with pressure of the exchange constant $\mathcal{J}$, which was discussed above to explain the enhancement of $\chi_m$ over $\chi_c$. From Eq. (8) and the PCM predicted values of $(1/\chi_c)(d\chi_c/dP)$, we obtain values of $(1/\mathcal{J})(d\mathcal{J}/dP)$. These are listed in Table I along with the values of $\mathcal{J}$ derived from Eq. (8). There are large errors associated with these quantities owing to the uncertainties noted above. However, the values of $(1/\mathcal{J})(d\mathcal{J}/dP)$ are quite similar for the Pr pnictides studied. The results of the pressure experiments will be discussed further in Sec. IV D.

#### *2. Tm pnictides (TmAs and TmSb)*

The general features of the Pr pnictide data are also evident in the data for the Tm pnictides, as can be seen from Table I. Although $\chi_m$ for the Tm pnictides is much larger than for the Pr pnictides, the enhancement and increase of $\bar{\eta}$ for both sets of pnictides are comparable.[24]

#### *3. Pr chalcogenides (PrS, PrSe, and PrTe)*

For this series of compounds the susceptibility appears to be slightly enhanced, but the values obtained are within the uncertainties of $\chi_c$. As can be seen in Table I, $\bar{\eta}$ decreases slightly with pressure, which is in qualitative agreement with the predictions of the PCM.

The data for PrS are anomalous in that $\bar{\eta}$ was found to be nonmonotonic with pressure. Two separate series of pressurization experiments on different pieces of the same sample showed that $\bar{\eta}$ decreased initially for pressures up to ~ 5 kbar and then increased with higher pressure. The data for both sets of runs are plotted in Fig. 8. Unfortunately, the available pressure is not large enough to indicate whether $\bar{\eta}$ continues to increase above 6 kbar. The reason for these peculiar results is not understood.

### D. Discussion

For the Pr and Tm pnictides the measured susceptibility is enhanced over the crystal-field-only

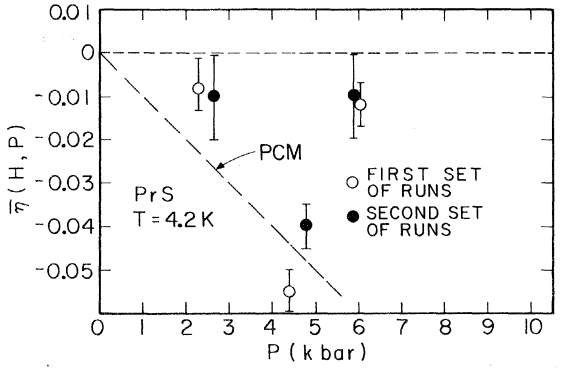


FIG. 8. Value of $\bar{\eta}$ at 4.2 K for PrS for two separate sets of runs of three high pressurizations each. Note the nonmonotonic behavior of $\bar{\eta}$ vs $P$ in contrast with the data of Fig. 7. Also indicated is the decrease of $\bar{\eta}$ with increasing $P$ predicted by the point-charge model.

value and *increases* with decreasing lattice constant, whereas the point-charge model predicts a *decrease*. We have discussed the results of these measurements in a purely phenomenological way, namely, by means of the pressure dependence of the exchange constant $\mathcal{J}$. Using this interpretation we obtain $(1/\mathcal{J})(d\mathcal{J}/dP)$, which is nearly equal for both Pr and Tm compounds. Based on a variety of experiments[25] the exchange constants for the rare earths are found to decrease with decreasing lattice constant for the light rare earths and to be nearly independent of lattice constant for the heavy rare earths. Therefore, we would expect $(1/\mathcal{J})(d\mathcal{J}/dP)$ to be significantly smaller for the Tm compounds. This discrepancy suggests that there may be other contributions to the observed pressure dependence of $\chi_m$ in addition to the pressure dependence of the exchange constant $\mathcal{J}$.

Several other mechanisms could contribute to the positive $(1/\bar{\eta})(d\bar{\eta}/dP)$ observed for the Pr and Tm pnictides. First, the effective charge on the nearest neighbors may change with pressure. Under these circumstances the pressure dependence of the susceptibility could be consistent with the PCM modified to include variations with pressure of the point charges [see Eq. (4)]. Second, it is possible that $x$ {which measures the relative magnitudes of the fourth- to sixth-order terms in the CEF Hamiltonian [Eq. (1)]} changes under pressure in a manner not predicted by the PCM. For example, in the Pr compounds a shift in $x$ of ~0.01 would produce an increase in susceptibility of ~3%. Regardless of the origin of the pressure dependence of $\chi_m$, it is interesting to extrapolate the results to find the pressure at which magnetic ordering should occur [divergence of the denominator of Eq. (8)]. For PrSb this is estimated to be ~80 kbar.

For the Pr chalcogenides the low-pressure de-

pendence of the susceptibility is qualitatively consistent with the predictions of the PCM. As noted above, at higher pressures the data for PrS become nonmonotonic. It is interesting to point out that, for this group of compounds, $\chi_m$ shows only small deviations from the crystal-field-only susceptibility. Thus we might expect the PCM calculations to give a good description of the pressure-dependent effects.

Very few pressure-dependent experiments exist for singlet-ground-state systems. In this paper we have presented the results of the pressure dependence of the susceptibility for a large number of these materials. In order to explain qualitatively the positive pressure dependence of the susceptibility of the Pr and Tm monopnictides, it would be useful to have independent measurements of other properties of these materials under pressure. For example, transport measurements under pressure may indicate whether charge is transferred with increasing pressure between the rare-earth ions and the pnictide ions (and/or whether the conduction-electron density changes under pressure). It should be noted that our results for the monopnictides are consistent with recent measurements of the pressure dependence of the Knight shift of $^{141}$Pr in PrP and $^{169}$Tm in TmP.[26] The results of the Knight-shift experiments showed a positive increase with pressure, whereas the PCM predicts a decrease. Although we have not studied the monophosphides, our results for the other monopnictides are all similar; we expect a positive pressure dependence of the susceptibility of the monophosphides will be found. Alternatively, it would be interesting to examine the pressure dependence of the Knight shift for some of the compounds reported in this paper.

## ACKNOWLEDGMENTS

We would like to thank Dr. W. M. Walsh, Jr. and Dr. H. C. Praddaude for several helpful discussions.

*Note added in proof*: The derivation of Eq. (7) does not require point charges. In order to derive $(1/\chi_c)(d\chi_c/dP)$ we merely require that the CEF Hamiltonian be described by Eq. (2) and that the symmetry of the CEF at all pressures maintain the symmetry of the lattice. It should be noted that Eq. (7) depends only on the LLW parameter $x$ (and not $W$).

---

*Supported by National Science Foundation Grant No. GH37141. Visiting Scientist, Francis Bitter National Magnet Laboratory, MIT, Cambridge, Mass. 02139.

†Supported by National Science Foundation and Temple University Grant-in-Aid.

‡Now at Physics Department, University of Konstanz, Postfach 733, D-775 Konstanz, Germany.

§Supported by the National Science Foundation.

[1]B. D. Rainford, K. C. Turberfield, G. Busch, and O. Vogt, J. Phys. C 1, 679 (1968).

[2]K. C. Turberfield, L. Passell, R. J. Birgeneau, and E. Bucher, J. Appl. Phys. 42, 1746 (1971). R. J. Birgeneau, E. Bucher, J. P. Maita, L. Passell, and K.C. Turberfield, Phys. Rev. B 8, 5345 (1973), and references cited therein.

[3]H. L. Davis and H. A. Mook, AIP Conf. Proc. 18, 1068 (1973).

[4]B. R. Cooper and O. Vogt, Phys. Rev. B 1, 1211 (1970).

[5]See P. Fulde and I. Peschel [Adv. Phys. 21, 1 (1972)] for an extensive review of the theory of crystalline-electric-field effects in metals.

[6]G. T. Trammell, Phys. Rev. 131, 932 (1963); B. Bleaney, Proc. R. Soc. A 276, 19 (1963); B. R. Cooper, Phys. Rev. 163, 444 (1967).

[7]K. Andres, E. Bucher, S. Darack, and J. P. Maita, Phys. Rev. B 6, 2716 (1972).

[8]E. Bucher, K. Andres, J. P. Maita, and G. W. Hull, Jr., Helv. Phys. Acta 41, 723 (1968).

[9]D. Davidov, R. Orbach, C. Rettori, L. J. Tao, and E. P. Chock, Phys. Rev. Lett. 28, 490 (1972); R. A. B. Devine, J.-M. Moret, W. Zingg, M. Peter, J. Ortelli, and D. Shaltiel, Solid State Commun. 10, 575 (1972).

[10]E. Umlauf, G. Pepperl, and A. Meyer, Phys. Rev. Lett. 30, 1173 (1973).

[11]M. T. Hutchings, in *Solid State Physics*, edited by F. Seitz and D. Turnbull (Academic, New York, 1964), Vol. XVI, p. 227.

[12]See, for example, J. M. Dixon and R. Dupree, J. Phys. F 1, 539 (1971).

[13]R. P. Guertin and S. Foner, Rev. Sci. Instrum. 45, 863 (1974).

[14]This clamp closely follows the design of D. Wohlleben and M. B. Maple [Rev. Sci. Instrum 42, 1573 (1971)]. Pure beryllium-copper is a special order from Kawecki Berylco Corp., Reading, Pa. 19603.

[15]S. Foner, Rev. Sci. Instrum. 30, 548 (1959).

[16]T. F. Smith, C. W. Chu, and M. B. Maple, Cryogenics 9, 53 (1969).

[17]R. J. Soulen, Jr., J. F. Schooley, and G. A. Evans, Jr., Rev. Sci. Instrum. 44, 1537 (1973).

[18]K. R. Lea, M. J. M. Leask, and W. P. Wolf, J. Phys. Chem. Solids 23, 1381 (1962).

[19]B. R. Cooper and O. Vogt, Phys. Rev. B 1, 1218 (1974).

[20]N. Berk (private communication).

[21]See also K. Andres, E. Bucher, S. Darack, and J. P. Maita, Phys. Rev. B 6, 2716 (1972).

[22]The compressibility $\kappa$ of PrSb was determined from elastic-constant measurements in this compound by M. E. Mullen, B. Lüthi, P. S. Wang, E. Bucher, L. D. Longinotti, J. P. Maita, and H. R. Ott [Phys. Rev. B 10, 186 (1974)]. The compressibilities of the other compounds were found from first linearly combining the compressibilities of the constituents and then scaling this value by the same factor obtained for the measured and calculated $\kappa$ for PrSb. The uncertainty in $\kappa$ for all samples other than PrSb is difficult to estimate, but is probably less than 25%.

[23]R. J. Gambino, D. E. Eastman, T. R. McGuire, V. L.

Moruzzi, and W. D. Grobman, J. Appl. Phys. 42, 1468 (1971). The susceptibility at room temperature of LaSb was found to be $\sim -5\times10^{-5}$ emu/mole. Using this as a rough order of magnitude of the background (band) susceptibility of our samples, we see that this is much less than $\chi_m - \chi_c$, so that we can ignore band and other small contributions to $\chi_m$ in our samples.

[24]We have also measured $\chi_m$ and $(1/\bar{\eta})(d\bar{\eta}/dP)$ for TmBi and found $\chi_m < \chi_c$ and $(1/\bar{\eta})(d\bar{\eta}/dP) \sim 0$. However, we believe the stoichiometry of this sample is questionable. Hence we do not regard the data as significant and have deleted the results from Table I.

[25]M. B. Maple, Solid State Commun. 8, 1915 (1970).

[26]H. T. Weaver and J. E. Schirber, AIP Conf. Proc. 24, 49 (1975).